SEVENTH FRAMEWORK PROGRAMME

THEME FP7-ICT-2009-C

Instrument	STREP
Project no.	244068
Project acronym	**CROSSTRAP**
Project title	**C**oherently-enhanced **R**aman **O**ne-beam **S**tandoff **S**pectroscopic **TR**acing of **A**irborne **P**ollutants

Deliverable D3.1

Development and characterization of an Yb gain module with cw laser diode pump power ≥ 700 W

Due date of deliverable	month 12
Actual submission date	01/03/2011
Start date of project	01/02/2010
Duration of the project	36 months
Organization name of lead contractor for this deliverable	**TU WIEN**
Dissemination Level	public

SHORT DESCRIPTION:

In Task 3.1 of WP3 the CROSS TRAP partners TU WIEN and LC are developing a 100-mJ level cw-pumped femtosecond Yb-doped solid-state amplifier. This deliverable reports on the development of the heart of that laser system—the gain module. This report analyzes the mechanical optical and spectroscopical properties of the gain medium, presents the design of the laser head and documents various tests that were needed to optimize the configuration. In addition, we provide an outlook how the system can be redesigned by taking advantage of a novel cooling unit developed in house and by applying the knowledge accumulated by trial and error during the first year of this research.

1_ INTRODUCTION 2

2_ CHARACTERIZATION OF YB:CaF_2 CRYSTALS FOR A MULTI-MJ CPA 3

3_ DESIGN OF THE LASER HEAD AND PUMPING CONFIGURATION 10

4_ ENVISAGED COOLING AND ARCHITECTURE IMPROVEMENTS 16

5_ CONCLUSIONS 20

6_ LITERATURE, PUBLICATIONS 21

1 INTRODUCTION

The main pump laser envisaged for the CROSS TRAP project should be based on modern diode-pumped solid state technology that ensures average power scalability, system robustness and compactness compatible with field applications. Previously, the CROSS TRAP consortium partners TU WIEN and LC have demonstrated a single-stage kHz-repetition-rate system delivering sub-200-fs pulses at 1030 nm with pulse energies up to 7 mJ. In Task 3.1, these two partners pursue the development of a booster amplifier based on the same gain material, Yb:CaF_2. Unlike the previous relatively straightforward development of the first-stage amplifier, the development of the booster faces substantially bigger challenges related, on the one hand, to the immature technology of high-average-power high-brightness laser diode stacks and, on the other hand, to the limitations of commercially available and practically meaningful cooling technology. In addition, the gain and thermal lensing requirements to a booster amplifier appear very different in comparison with the forgiving regenerative amplifier configuration used in the first stage.

2_ CHARACTERIZATION OF YB:CaF_2 CRYSTALS FOR A MULTI-MJ CPA

Yb-doped fluorides represent a very attractive class of laser materials for multimillijoule CPA systems [Cam07, Dou07, Luc04, Sie07, Sie08, Sie09] because of their transparency in a wide wavelength region from the VUV to the IR; low linear and nonlinear refractive indices and low nonradiative relaxation between adjacent energy levels. Among different fluoride hosts, CaF_2—one of the first host materials since the early 1960s [Sor60, Boy62] and the very first host material to be used with direct diode pumping at cryogenic temperatures [Key64]—has one of the lowest phonon frequencies (328 cm^{-1}) and a high thermal conductivity (around 10 Wm-1K-1 at room temperature and 39 $Wm^{-1}K^{-1}$ at 83 K [Web03]). Recently, a modified host, Yb3+,Na+:CaF2 was introduced, where Na+ has been suggested to act as a charge compensator in CaF_2[Su05, Su05a]. It was shown in [Su05] co-doping with Na+ leads to significant modifications of the spectroscopic properties, especially to an increase of the radiative lifetime.

For today there is a number of crystal growers which supply Yb doped CaF_2 crystals. However in the community of the developers of Yb:CaF_2 CPA systems there is a variety of opinions about the optimal concentration of Yb, role of co-doping, and optical quality of Yb:CaF_2 crystals from various suppliers. In order to make a right choice of the crystal for our CPA system under development we have evaluated absorption and luminescence of Yb:CaF_2 crystals having different Yb doping and Na co-doping concentrations and purchased from four different crystal suppliers, namely, Shanghai Institute of Ceramics, Chinese Academy of Sciences, China (SIC), Eksma Optics (EKSMA), Lithuania, Korth Kristalle GmbH (KORTH), Germany and Hellma Materials GmbH & Co. KG (HELMA), Germany. The absorption spectra of various crystals were recorded using UV-VIS-NIR spectrophotometer (VARIAN CARY 5G). The luminescence spectra were recorded by the optical spectrum analyzer (AQ 6315A, Yokogawa). The excitation source was a single-emitter 975-nm laser diode operating n the cw mode. The crystals have been placed at a fixed position in order to have similar measurement conditions and to be able to compare relative intensities of the luminescence for different crystals. The measurements have been performed at room temperature.

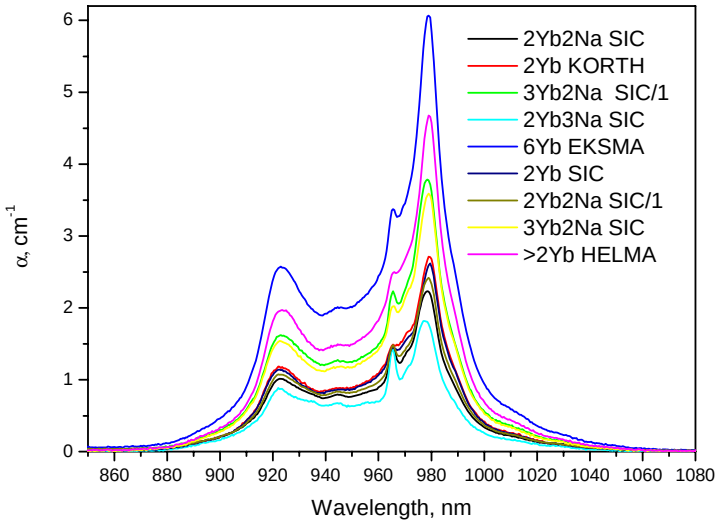

Fig.1 Absorption spectra of various Yb-doped and Na co-doped CaF_2 crystals. Numbers before Yb and Na indicate molar percentage concentration as specified by the crystal suppliers (indicated I the figure).

As can be seen from Fig.1 absorption of Yb(Na):CaF_2 crystals scales with Yb concentration, i.e. it increases with increasing of Yb content. It is also obvious that Na co-doping lowers absorption strength for given Yb concentration as it was reported earlier [Pug09]. However absorption of the crystals with the same specified Yb concentration varies within rather broad range. This might be attributed to both, different crystal composition due to differences in growth process and to imprecise Yb concentration determination. The later is more probable reason since the shape of the absorption spectrum stays practically invariant for both, Yb:CaF_2 and Yb,Na:CaF_2 groups of the crystals.

Luminescence spectra presented in Fig. 2 were measured at identical conditions (by keeping the same excitation power and placing the crystal at exactly the same position with respect to the pump source and to the detection system). In addition measured spectra were scaled with respect to the absorbed pump power and were corrected by taking into account the re-absorption. This allows us to compare luminescence efficiency in the near infrared spectral range for different crystals. Resulting spectra reveal that within small margins majority of the crystals exhibit similar luminescence strength. In addition the shapes of the luminescence spectra remain practically unchanged. As an exception from this general trend the crystals with 3%Yb2%Na, 2% Yb and 2%Yb3% Na, all from SIC, should be mentioned. The fact that other crystals from the same supplier and crystals with the similar Yb and Na contents fall into the general trend reveals that most probably crystal growth irregularities is the main cause for the deviation.

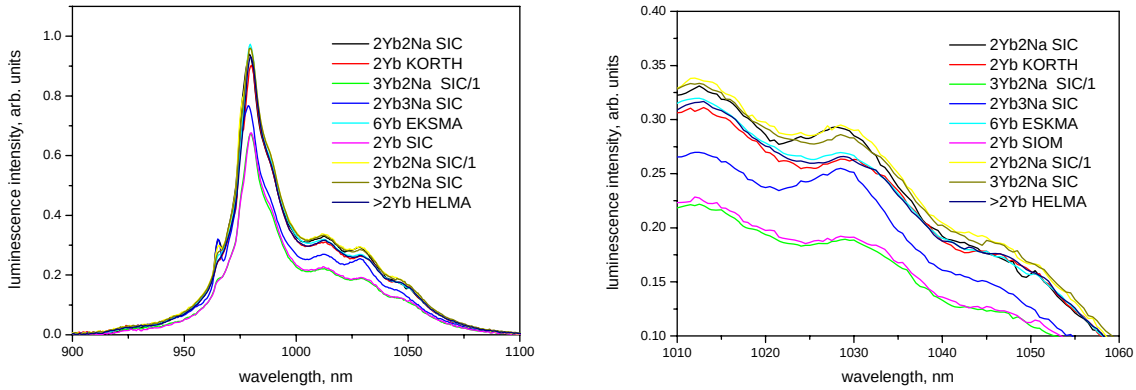

Fig.2 Right: scaled luminescence spectra (for details see text) of various Yb-doped and Na codoped CaF_2 crystals. Numbers before Yb and Na indicate molar percentage concentration as specified by the crystal suppliers (indicated I the figure).Left: luminescence spectra zoomed in the spectral region 1010-1060 nm corresponding to the spectral range of laser/amplifier operation.

Since Yb(Na):CaF_2 in general is a low-gain material one needs to use either long or high-dopant-concentration crystals for extraction of substantial amount of energy from the amplifier. Due to limited beam quality of multi-bar diode stacks long laser crystals can be used only in the case of transversal pumping (this pumping geometry is described in the next section). For longitudinal pumping of long crystals high brightness good mode quality pump source is required, such as the recently developed high spatial quality fiber laser [Bou08]. Although this type of laser to the date is limited in the output power to 50 W, we have performed experiments with various crystals in order to investigate potential of longitudinal pumping in Yb(Na):CaF_2 amplifier based on a long laser crystal. Experiments have been performed at room temperature. The results of the experiments look rather promising. First of all, due to high beam quality (M^2=1.3) pump radiation can be focused rather tight by using long focal length lens providing high brightness over a relatively long distance. This leads to the induced transparency in the laser crystal which allows homogeneous pumped channel in rather long or (and) heavily doped crystals. The optical density as a function of pump power of each crystal is summarized in Fig. 3. The highest absorption reduction level was observed in 6% doped CaF_2 crystal. Optical density decreases from 0.97 to 0.2 when increasing pump power to 38W. Since the OD directly scales with the unexcited Yb^{3+} ion concentration, it becomes possible to estimate the population inversion at different pump levels. High brightness pump source in this case allows decreasing number of unexcited ytterbium sites by ~80 % which corresponds to 7.72×10^{20} cm^{-3} population inversion density. Moreover, as it can be seen from Fig. 3, lower doping level Yb^{3+} crystals exhibit smaller optical density changes at the same pump power range. This behavior can be explained by the electron population dynamics and absorption

saturation effect in a two energy level system. Since, highly doped Yb^{3+} crystals require a higher intensity for reaching the absorption saturation, higher population inversion density can be obtained in this case.

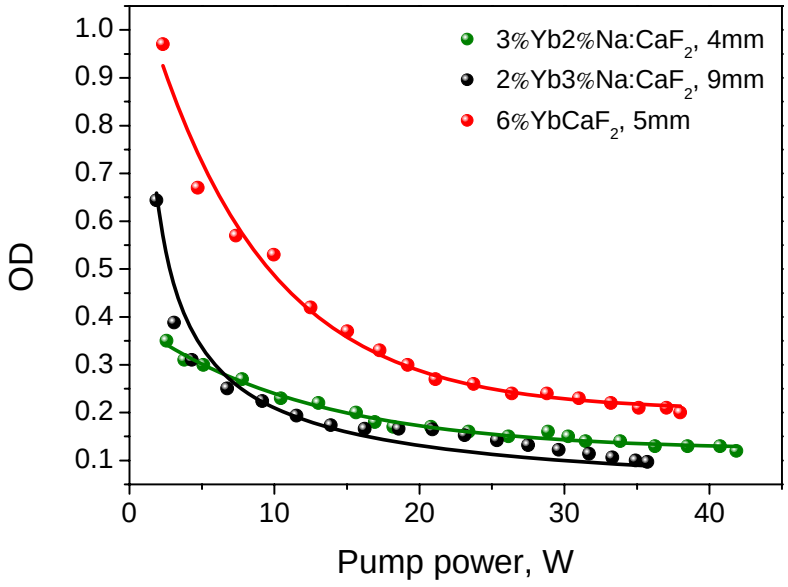

Fig. 3. Dependence of the optical density on pump power of different Yb^{3+} doped crystals.

According to the experimental results, the high brightness pump radiation, induces the transparency in the initial segment of the crystal and remains sufficiently intense to create inversion further. This allows spreading the parasitic heat over a longer crystal length and reducing the thermal load per unit volume. A price for this advantage is low pump absorption efficiency. Photo induced bleaching was clearly observed in all type of crystals, because pump wavelength of the present source very well matches the ZPL region, causing the highest available population inversion of only 50%. The situation is supposed to improve by cooling the crystal to cryogenic temperatures (see next section) and by tuning the wavelength of the pump source out of the region of zero phonon line.

The results of small-signal-gain measurements are even more striking: an unexpectedly for Yb:CaF_2 high gain of 3.2 has been measured in the case of 6%-Yb-doped, 1-cm long Yb:CaF_2 crystal (Fig. 4).

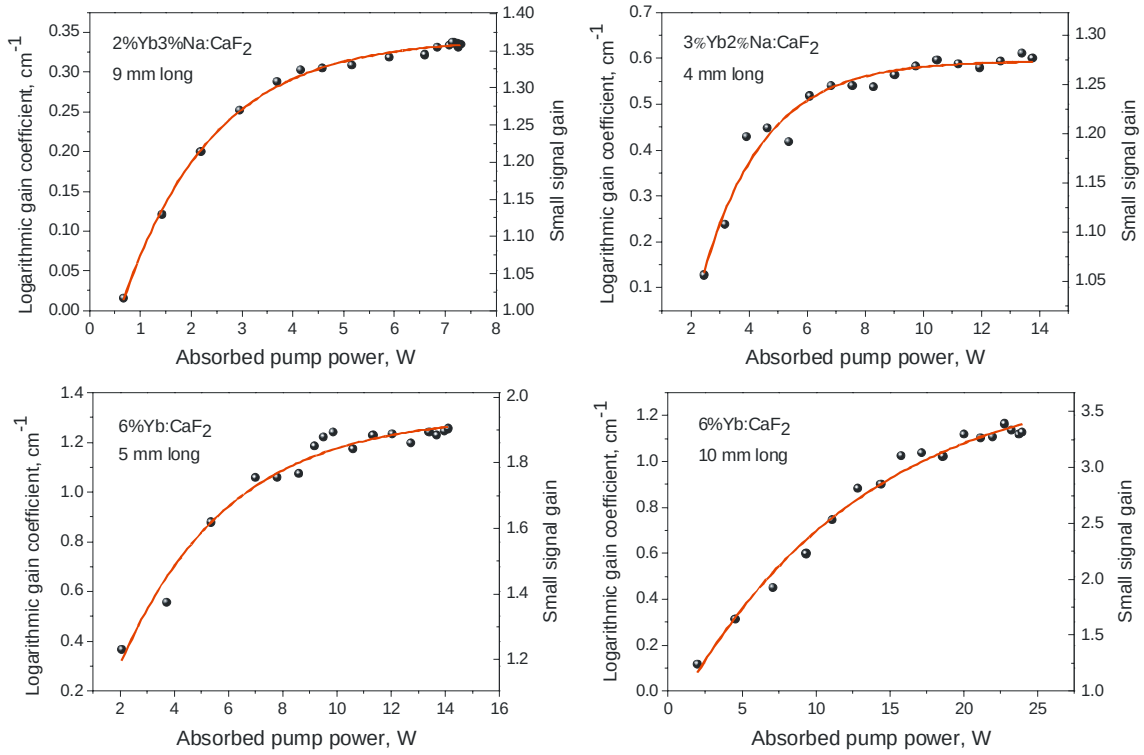

Fig. 4. Small signal gain as a function of absorbed pump power of different Yb^{3+} doping level crystals, measured at 1030nm.

Since increased concentration of Yb in CaF_2 crystal might lead to modification of optical and thermal properties we have investigated 6% Yb doped CaF_2 crystal at room and cryogenic temperatures. Rom temperature absorption and emission spectra (Fig 1 and 2) revealed no changes in the lineshape as compared to the crystals having lower dopant concentration. Absorption and emission spectra of 6%Yb CaF_2 and 2%Yb,2%Na:CaF_2 crystals measured at 110K temperature are given in Fig. 5. As one can see from the figure the absorption spectrum of 2%Yb,2%Na:CaF_2 has special features, namely slightly higher absorption at around 920 nm, more pronounced absorption band centered at 962.5 nm and a broadened shoulder at around 976 nm, to the blue side from ZPL. All those features are characteristic for Na co-doping and have been reported in [Pug09]. For the rest absorption spectra of both crystals look rather similar indicating that relatively high concentration of Yb does not influence the absorption of 6%Yb CaF_2 crystal much. Luminescence spectra of both crystals reveal luminescence bands located at the same wavelength although relative intensity of the bands is a bit different. Especially important feature of 6%Yb CaF_2 crystal is higher luminescence intensity to the blue from 1030 nm, which suggests that the crystal has potentially larger amplification bandwidth at low temperatures as compared to the case of

2%Yb,2%Na:CaF_2 crystal. A possible reason for broader luminescence is larger disorder because of high concentration of Yb. Although this might be beneficial from the point of view of the amplification bandwidth it might act negatively on the thermal properties of the crystal: decreased thermal conductivity leads to both, increased thermal lens and thermally induced birefringence.

Another potential drawback of high Yb doping is increased inhomogeneity of the crystal. In order to check that we have mapped absorption spectra of 6%Yb CaF_2 through the area of 5×10 mm.

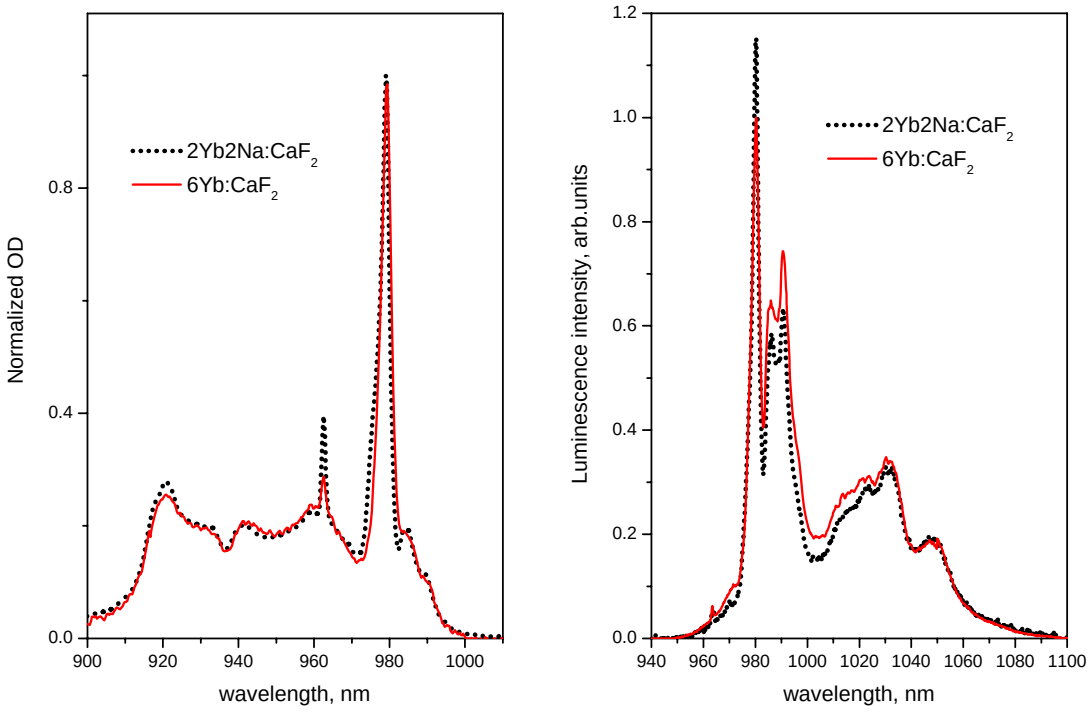

Fig.5. Absorption (left) and emission (right) spectra of 6%Yb CaF_2 (red solid line) and 2%Yb,2%Na:CaF_2 (black dotted line) crystals measured at 110K temperature.

Figure 6 shows in schematics of the measurement setup used for recording the transmission spectrum at a localized point on the crystal's surface at room temperature. The light source, a white light, tungsten halogen lamp from Ocean Optics Inc., was focused on the crystal's front-face into a beam measuring approximately *1mm* in diameter. A spectrometer, USB2000 from Ocean Optics Inc., recorded the entering light's intensity spectrum I_{out} and calculated $T(\lambda)$ by taking the lamp's prerecorded intensity I_{in} spectrum as reference. In order to ascertain the homogeneity of the crystal, the measurement was iterated, scanning the crystal's surface at various points labeled 1-24.

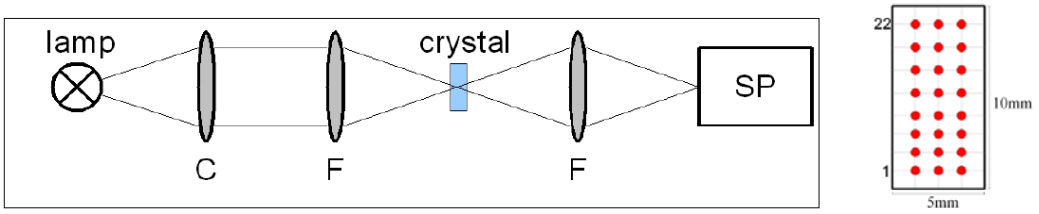

Fig. 6. Transmission spectroscopy setup at room temperature, with white-light lamp as a source, collimating lens C, focusing lenses F, and spectrometer SP.

The resultant map on the crystal's doping homogeneity is illustrated in Fig. 7 and reveals that the doping profile slants towards one corner of the crystal. This effect most probably is caused by the gradual decrease of Yb concentration during crystal grows process. A variation of the doping concentration from 1.79×10^{21} cm^{-3} to 1.92×10^{21} cm^{-3} has been estimated which amounts in nearly 9 % variation of the Yb concentration.

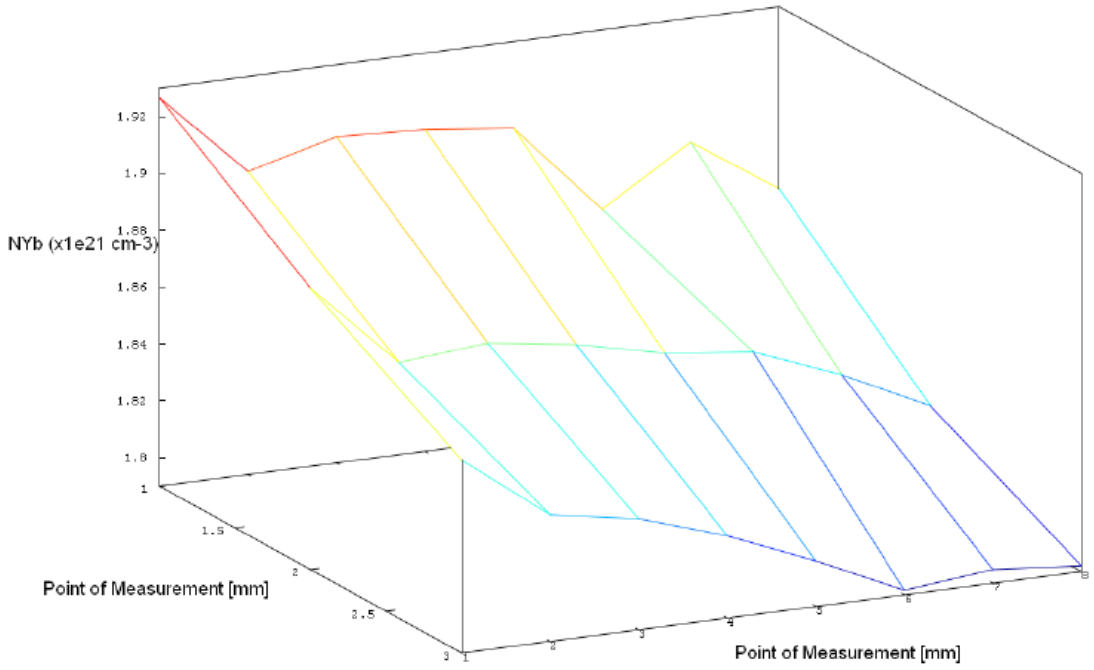

Fig.7 Measurements of Yb doping homogeneity in 6% Yb:CaF_2 crystal.

Next to the increased gain cross-section cooling of the laser crystal to cryogenic temperatures makes laser or amplifier more efficient due to the decreased ground state absorption (GSA) at lasing wavelength (Pug 09) as well as improves thermal properties of the crystal [Web 03] leading to lower thermal lens and thermally induced birefringence. Modification of the absorption spectrum and gain cross-section with decreasing temperature for 2%Yb,2%Na:CaF_2 crystal are presented in Fig.8. The cooling of the crystal to cryogenic temperatures leads to the disappearance of GSA in the spectral region above 1000 nm and to a substantial

increase of the emission and absorption cross-sections, providing the potential for a high-efficiency pumping and energy extraction from the amplifier crystal (Pug 09).

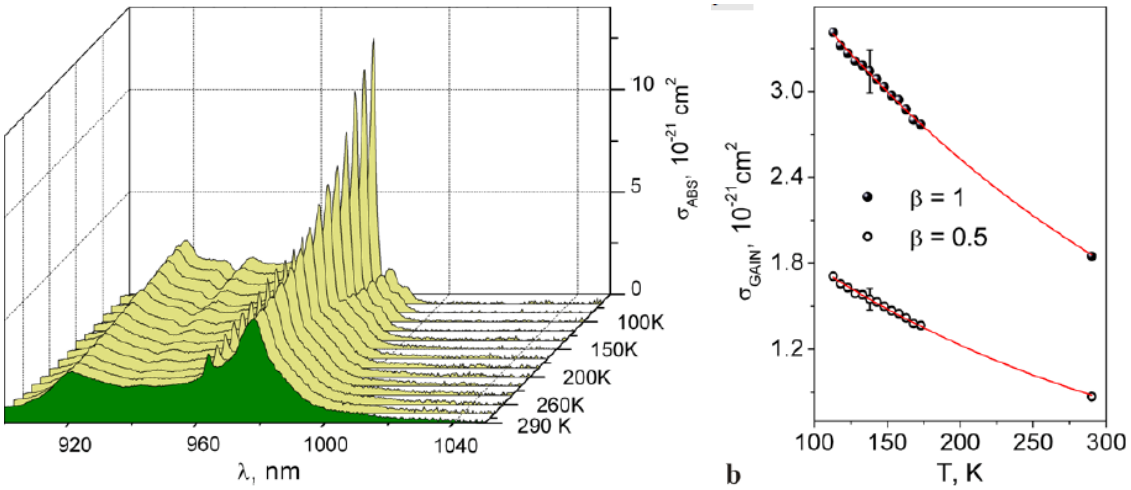

Fig.8. Left: evolution of the absorption spectrum of Yb:CaF_2 crystal with decreasing temperature. Right: dependence of gain cross-section on temperature for two fractions of the excited state population.

However as one can see from the Fig. 9 although spectrum of the emission cross-section in the vicinity of 1030 nm (spectral region where Yb:CaF_2 laser systems operate) does not narrow substantially providing amplification of broadband radiation supporting sub-200 fs pulse duration (Pug09a), the absorption spectrum in the vicinity of zero phonon line (ZPL) gets rather narrow. This puts certain limitations on the spectral properties of the laser diodes which are used to pump the laser crystal in the amplifier.

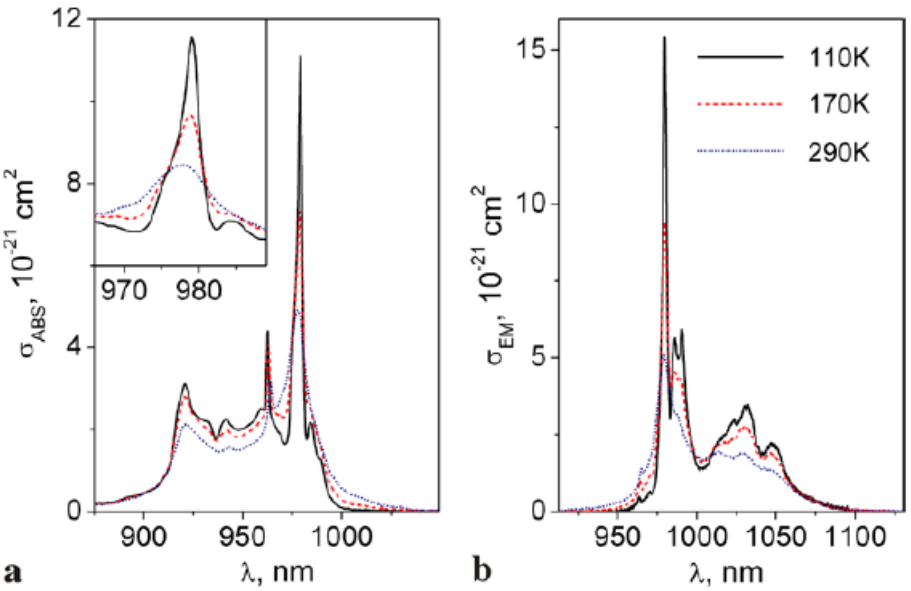

Fig. 9. Absorption (a) and emission (b) cross-sections of Yb:CaF_2 crystal at temperatures of 110 K (solid line), 170 K (dashed line) and 290 K (dotted line). In the inset to panel (a), the absorption cross-section is zoomed in the vicinity of the ZPL.

3_ DESIGN OF THE LASER HEAD AND PUMPING CONFIGURATION

Because of the low quantum defect, high quantum yield, suitability for direct diode pumping and a large fractional gain bandwidth, Yb-doped hosts dominate the effort to develop high-repetition-rate, high-average power femtosecond amplifiers for a variety of industrial and research applications. Although Yb crystals generally exhibit very long fluorescence lifetimes, frequently longer than 1 ms, obtaining high gain is very challenging because their emission cross-section is 20—30 times lower than that of Nd and Ti:sapphire [Krup00]. Very high laser saturation and pumsp saturation intensities (e.g. for Yb:KGW and Yb:YAG ~10 kW/cm^2 and ~30 kW/cm^2, respectively) require an exceptionally tight diameter of the pump [Fan90] and cavity modes. Suitably broadband-gain Yb crystalline materials that are most promising for high-energy femtosecond amplification (Yb:CaF_2, Yb:KGW/KYW, Yb:GSO/GYSO) can be pumped into the ZPL around 977 nm thus providing the smallest possible excretion of parasitic heat for 1.0-1.03-μm amplifier operation. One of the challenges with using this pump wavelength is the requirement for a narrow precisely controlled linewidth of the pump light, dictated by the necessity, on the one hand, to couple into a narrow blue shoulder of the ZPL and, on the other hand, to avoid spectral overlap with the ZPL peak in order not to lower the amplifier efficiency. Recent progress in developing VBG-stabilized laser diode bars at 977±3 nm has made such efficient pumping schemes possible. The need for a high-brightness pump for Yb lasers has led to spectacular achievements in the power scaling of an individual laser diode emitter and in the brightness increase of a diode bar through the use of micro-optics and improvements in the diode mechanical tolerances. Despite this progress in the diode bar technology, the beam quality from the best available diode bars and all the more from diode stacks remains vastly inferior to the laser mode, indicating that accurate mode matching distance between the pump volume and the laser mode in an Yb-doped medium will be very short, ranging, depending on the tightness of the pump focus from sub-mm to several mm. The inability to sustain high pump brightness required for operation near the pump saturation intensity limits the choice of pump configurations to (Fig.10):

• thin-disk/active mirror with re-circulating pump. It is highly suitable for KW output power generation but very impractical for amplification in view of a low-single pass gain. (L_{Gain}≤0.2 mm)

• slab with a rectangular pump mode. (e.g. INNOSLAB by ILT in Aachen L_{Gain}<10 mm).

• end-pumping of a cryogenically cooled crystal [Rip05] (L_{Gain}>10 mm).

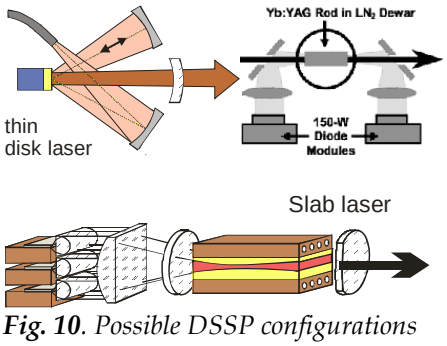

***Fig. 10**. Possible DSSP configurations*

The extension of the gain length in the cryocooled version is determined by the fact that (a) at low temperatures ground state absorption (GSA) is suppressed and (b) that the saturation intensity is lower. At room temperature, poorly pumped crystal ends exposed to divergent pump light would contribute losses due to GSA, not gain.

Our proposed booster amplifier configuration schematically shown in Fig. 11 is based on a hybrid edge-pumped slab approach. This design combines the advantages of the slab configuration (in terms of a high longitudinal gain) and the thin disk laser (in terms of multipass pump beam recirculation. In the proposed design, the pump beam can be reimaged into the 1.5-mm-thick crystal up to 4 times, making it in total 8 passes (4 double passes) through the crystal. Depending on the doping level, 40-50% of the incident pump power at ~976 nm is absorbed in a single bounce (double pass) on a 1.5-mm-thick crystal. Therefore just a few passes are already sufficient to reach a highly efficient pump absorption.

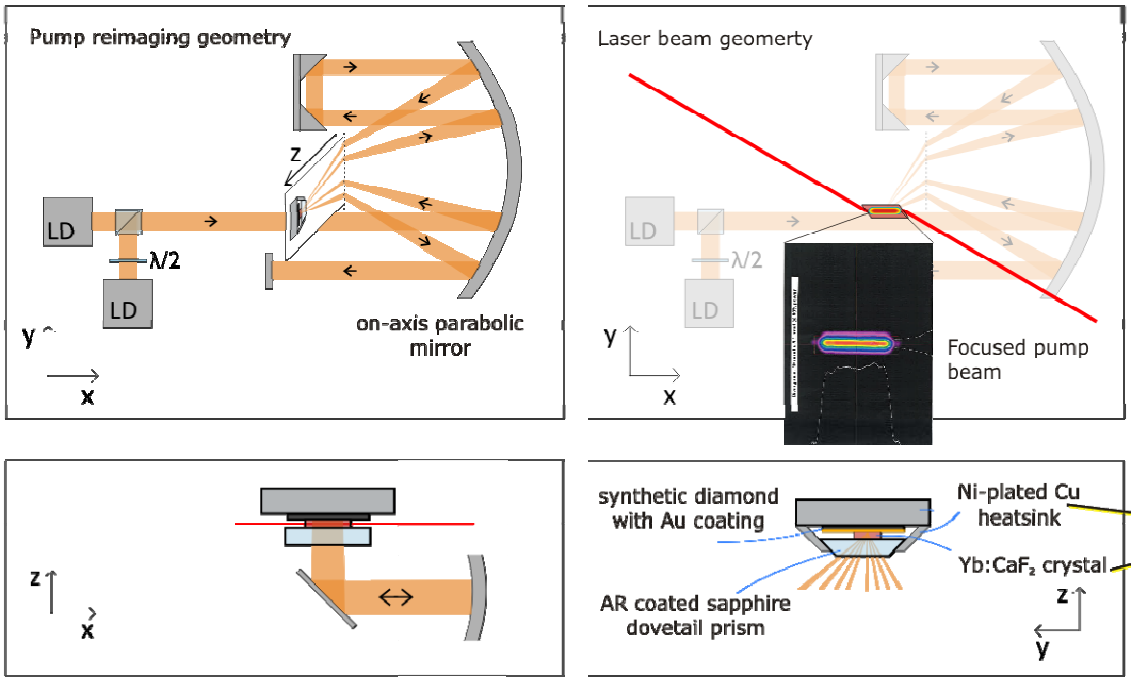

Fig. 11. Multipass pumping configuration with two 350-W laser polarization-combined diode stacks.

The main reason for this untraditional pumping configuration is the lack of appropriately bright laser diodes. Whereas radiation from a single laser diode bar, typically consisting of 19 emitters producing 50-60 W can be shaped into a high-quality nearly circular pump spot by applying slow axis collimators, this approach is not suitable for systems generating hundreds of watts of 980-nm pump light. In our design we have opted for micro-lensed laser diode stacks which are commercially available from DILAS and some other manufacturers. The beam profile of a 350-W 976-nm DILAS diode stack focused onto the Yb:CaF_2 crystal is reproduced in Fig. 12. It is evident that in one direction the beam from the stack can

be focused tightly just like in the case of a single bar. The orthogonal, poorly focusable coordinate is aligned along the laser crystal in such a way that the amplified laser beam interacts with the entire length of the inverted crystal volume. In this way the poor focusing of the pump beam in the longitudinal direction of the amplifier seed beam becomes unimportant and permits increasing the gain length.

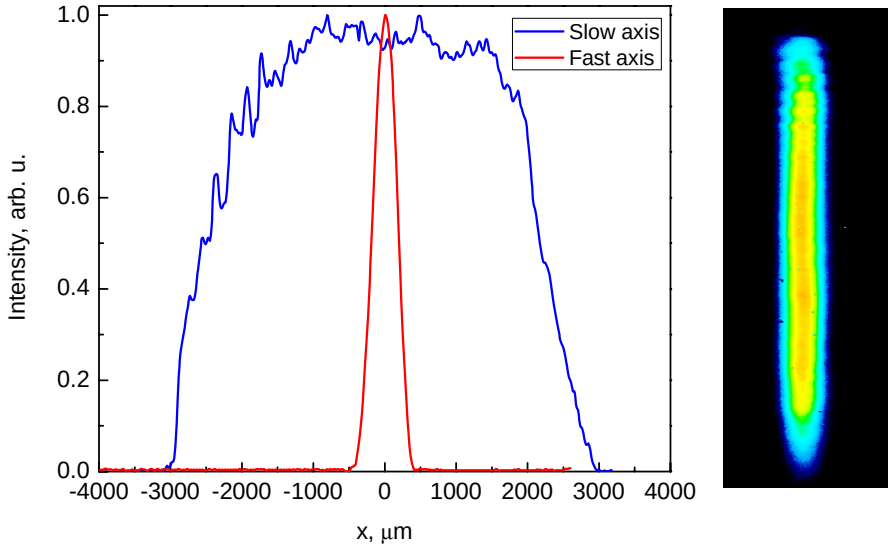

Fig. 12. Beam profile at 1/e² level as focused with f=200 mm spherical lens together with f=400 mm focal length lens in front in order to increase the width of the beam spot size in the slow axis direction. fast axis 612 µm; slow axis 5600 µm.

The developed gain module arrangement consisting of a vacuum chamber, commercial cryogenic cooler (Cryomech PT-90), two 350-W pump laser diodes and the pump reimaging optics are shown in Fig. 13.

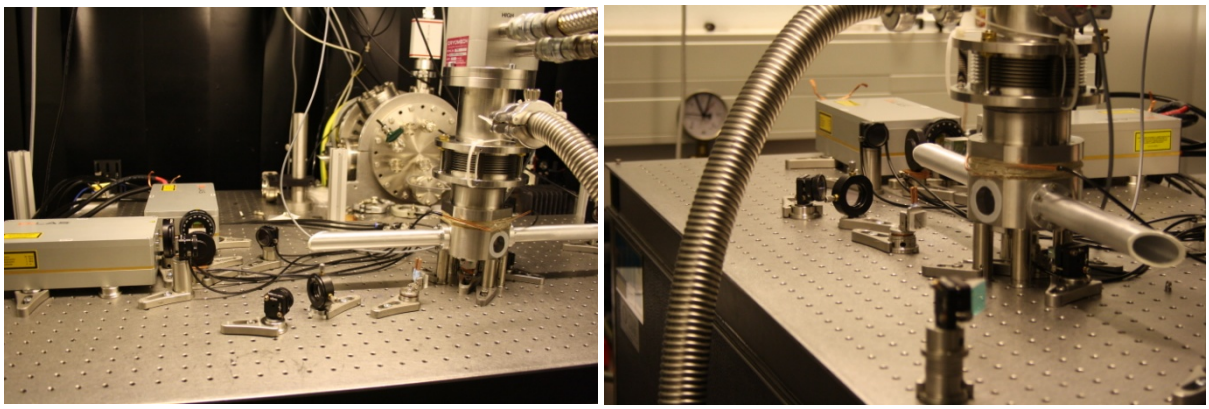

Fig. 13. Photographs of the cryogenically cooled Yb:CaF_2 booster amplifier head in the TU WIEN lab.

One of the successfully addressed major challenges in the development of a broadband Yb-doped cw-pumped gain module is the geometry of the laser crystal and the mounting of the crystal on the cold head. Initially, we have worked with Brewster-cut slab crystals that were 5×1.5 mm in cross-section and approximately 9 mm long. Our tests have shown that crystals of this geometry are easily thermally destroyed in the edge-pumped configuration due to the bulging of the crystal under

the pump which leads to a loss of thermal contact with the heat sink. This issue was solved by switching to 1.5×1.5 mm cross-section crystals which turned out to be significantly more robust with regard to thermal shock. However this highly inconvenient crystal geometry has created a problem of crystal mounting. Two different approaches to clamp the crystal have been investigated: side cooling (Fig. 14, left) and top—bottom cooling (Fig. 14, right). The clamping geometry refers to the direction of the pump laser diode beam incident perpendicularly to the plane of the crystal mount.

Fig. 14. Different laser crystal clamping methods. Left: side clamping. Right: top—bottom clamping. The conductive cooling from the top in the configuration on the right is supplied via an AR-coated sapphire prism which is bonded on an optical contact to the gain crystal. The cooling from the bottom is provided by a Au-pated diamond plate soldered to the copper heatsink. The model on the left shows a newer, 1.5×1.5 mm cross-section crystal, whereas the model on the right shows the original 5×1.5 mm type. The diameter of the outer disk is 70.6 mm.

Thermally-induced stress depolarization, thermal lens and gain properties in both clamping geometries were tested under identical conditions with identical 1.5×1.5 mm cross-section crystals from the same batch. After optimizing the crystal insertion process and introducing a thermal annealing process, it was possible to eliminate crystal cracking under the available amount of optical pump. Negative thermal lens in the direction of the cooling was observed in both clamping geometries but it was approximately 5 times stronger in the case of side clamping. We explain this large difference by the fact that the heat flow gradient in the side-clamping configuration is perpendicular to the pump beam, whereas in the case of top—bottom (or face and back) cooling the thermal gradient is parallel to the pump beam. Consequently, the temperature of the hottest part of the crystal, the input face, is significantly lower as compared to the case when the entire amount of heat has to be transported to the sides of the crystal. The top—bottom cooling geometry has produced very encouraging results in terms of thermally-induced depolarization and thermal lens. The onset of weak thermal lensing with the increase of the pump diode current is presented in Fig. 15.

As explained in detail in sec. 2, precise diode linewidth matching to the absorption spectrum of Yb:CaF2 is required at the cryogenic pumping conditions because of the narrowing of the zero phonon line. To satisfy this demand, the laser diode stack have been ordered with volume Bragg grating (VBG) stabilization of the emitted wavelength (target λ=976.6 nm).

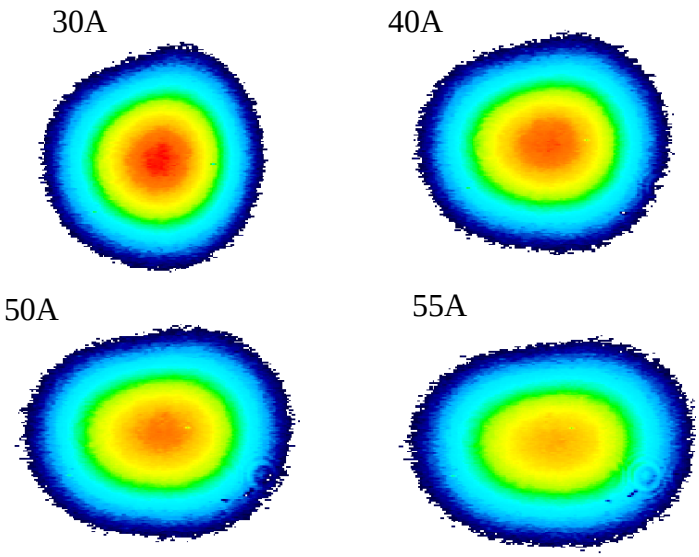

Fig. 15. Formation of a weak thermal lens probed with a ∅~1-mm pilot beam at 1030 nm as a function of applied laser diode current (60 A corresponds to ~350 W of incident pump per laser diode stack).

Figure 16 compares the emitted line width for a conventional single diode bar and a VBG-stabilized stack. In addition, Fg. 16 shows the dependence of the line width on the cooling water temperature, suggesting that it is difficult to attain optimum line width for both 350-W pump modules simultaneously if they are connected to the same water chiller.

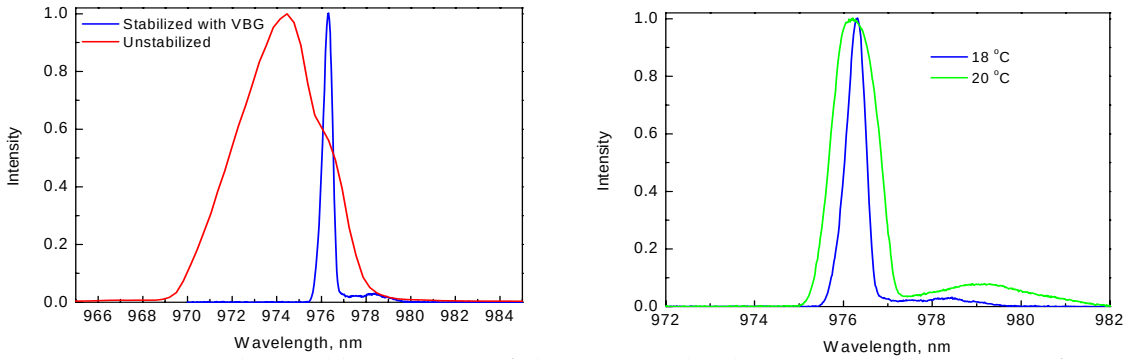

Fig. 16. Emission line width narrowing of the pump diodes due to VBG stabilization. Left: spectra of a conventional diode bar and of a VBG-stabilized stack. Right: strong dependence of the resultant line width on the temperature of the cooling water supplied to the VBG-stabilized stack.

The target unsaturated single-pass gain of the system under development is expected to reach ~2. The current highest value obtained with a single pump bounce on the crystal is already 1.48 for a 200-mm pump focusing lens (cf. Fig. 12) and should increase in the multi-pass pumping configuration. Preliminary results of small signal gain measurement are shown in Fig. 17. They indicate that gain undergoes saturation regardless of the length of the pumped volume. However this "saturation" is an artifact caused by cooling problems—the drop in the gain corresponds to a rapid warming up of the cold finger inside the close-loop refrigerator. The disruption of the cooling occurs when the Cryomech cooling unit it driven to the top of its cooling capacity, roughly 90 W. We have devised measures to shield the cold finger and the crystal mount from the scattered light (pump and

amplified spontaneous emission) which is absorbed by uncoated or poorly coated copper parts and causes a rapid increase of the heat deposited on the cold finger.

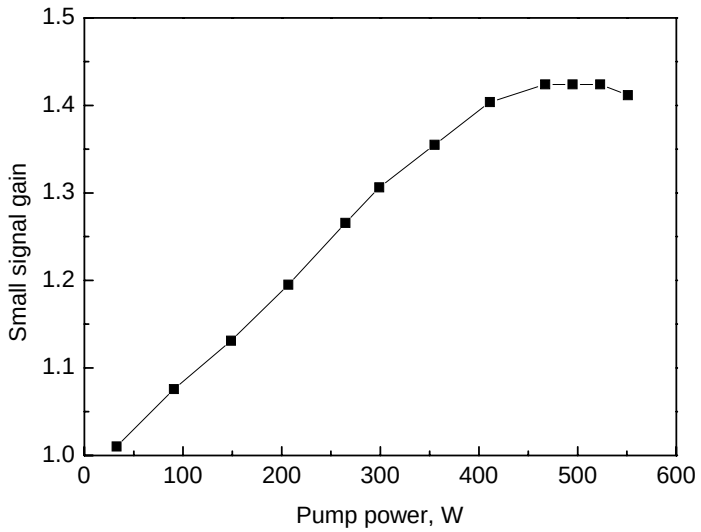

Fig 17. Small signal gain measurement vs incident pump power. About 40% of the incident pump power is absorbed in a double pass through the 1.5-mm-thick crystal. Note that the apparent gain roll-off at high pump powers is caused by the temperature increase of the cold finger and the crystal holder assembly.

4_ ENVISAGED COOLING AND ARCHITECTURE IMPROVEMENTS

In the initial phase of the project we have relied on a commercial cooling unit (Cryomech) because it could be purchased of the shelf. However, such a unit is not optimal for field applications because of its size, complexity (cf. Fig. 13) and unnecessarily low cooling temperature. Although the use of helium as a refrigerant permits reaching very low temperatures, the principal disadvantage of in this cooling method lies in a very low thermal conductivity of the noble gas. As a result, a mechanical piston has to be incorporated directly in the cooling head which makes the entire setup very bulky and introduces vibration on the laser crystal. We have examined the possibility to develop a dedicated cooling unit that would not reach deep cryogenic temperatures but, instead, would allow a higher heat load and operate at a temperature optimal for broadband amplification in Yb:CaF_2. An additional concern is to make the cooling head very compact to fully insert it into a miniature vacuum chamber.

Below we review the design considerations for an optimal cooling unit for the envisaged gain module Most cryo-cooled laser systems operate at temperatures close to the temperature of liquid nitrogen (LN2), i.e. around 77K. In the case of Yb:CaF, a semi-cryogenic temperature of 110K to 135K is sufficient to fulfill all physical requirements (heat conductivity, dn/dT, 3-4 level system, absorption bands, cf. sec.2) to use Yb:CaF crystal as a high power laser gain medium. As reported in sec. 3 (Fig.17), the heat load on the cold head reaches the operating limits of a conventional cooling system when the pump power reaches several hundred watts.

The requirements to a custom-designed cooling system can be summarized as follows:

- Cooling power >100W
- Vibration free operation of the cold head
- Orientation independent operation
- Temperature regime 110K-135K
- Compact cold head
- A single flexible coolant delivery hose/tube.

Different cooling methods were investigated:

1. Gifford-McMahon
2. Pulse-Tube –Refrigeration
3. Vapour– compression refrigeration
4. Vapour-compression cascade refrigeration
5. Joule-Thomson –Refrigeration

Pulse Tube Cryocoolers vs. Gifford-McMahon Cryocoolers

Three main differences exist between Pulse Tube (PT) cryocoolers and Gifford-McMahon (GM) cryocoolers (Fig. 18).

a.) Price: In general, GM cryocoolers are less expensive than PT cryocoolers of similar cooling power.

b.) Vibration: Both GM and PT cryocoolers are mechanical refrigerators that do have some level of vibration. These vibrations are caused by shifting the working gas (He) through the regenerator.

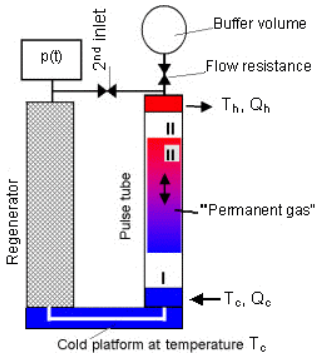

Fig. 18. Left: GM cryocooler head; Midle: PT cryocooler head; Right: PT operation cycle.

c.) Orientation The performance of PT cryocoolers (middle picture- cold head) is orientation-dependent. PT cryocoolers only function properly when they are operated in a purely vertical orientation. GM cryocoolers (left picture- cold head) will lose some cooling power when the cold head is not operated vertically, but the base temperature will not be affected. GM cryocoolers can operate in any orientation. The room temperature mounting flange provides the interface for a vacuum shroud or vacuum chamber. Vibrations at the room temperature mounting flange will be transmitted to the vacuum shroud and anything else the shroud is physically contacting.

When a cryocooler is attached to a delicate instrument like high power laser, a PT system presents a better choice than a GM system because the vibration level at the

room temperature mounting flange and the cold head of a PT system are significantly lower than in a GM system. GM cold heads have vibrations on the order of 50 microns along the axis of the cold head. GM cold heads have vibrations on the order of 10 microns perpendicular to the axis of the cold head. Pulse tube cold heads have vibrations on the order of 10 microns along the axis of the cold head and 3 microns perpendicular to the axis of the cold head. Unlike GM cold heads, PT cold heads do not have any internal moving parts to add to vibration levels of the cold head. The valve motor on GM cold heads is always bolted to this room temperature mounting flange. As the motor turns, the valve is opened and closed. The vibrations from this valve motor will contribute to the overall level of vibrations of the cold head. The movement of the displacers may also contribute to the vibrations at this flange on a GM cold head. The valve motor on some PT cold heads does have moving parts to open and close the rotary valve, although a "remote valve option" is available. This allows the valve motor to be mounted externally from the cold head, reducing vibrations from the motor.

d.) Cooling Power. GM cryocoolers are available up to 600W @ 80K but the high vibration level makes this cryocooler unfeasible for phase-stabilized laser systems. PT cryocoolers (e.g. Cryomech PT-90 described in sec. 3) are available up to 75W @ 80K cooling power which is at the very limit for the projected laser system.

Vapour-compression cascade refrigeration vs. Joule-Thomson –Refrigeration

Higher temperature (130K) makes it possible to adopt cascade refrigeration methods or Joule-Thomson- methods. The big advantage of this method is the constant flux of refrigeration which is pumped through the cold head. This leads to a vibration-free operation inside the vacuum chamber. Another big advantage compared to GM, PT cryocoolers is the high cooling density. Thereby the size of the cold head can be reduced. The basic principle is well known from commercial domestic refrigerators. Gas, e.g R404A, is compressed by a compressor and cooled to ambient temperature (condenser)- this procedure leads to condensation of the gas. The expansion valve reduces the pressure and the liquid gas is vaporized. The change of aggregate state leads to a very high cooling capacity. This method can be cascaded with several cooling cycles and gases.

Each gas can be liquefied at a specific pressure and temperature:
In the 1st cycle, R404A is liquefied and expanded -> 243K
In the 2nd cycle, R23 is liquefied and expanded-> 191K
In the 3rd cycle, R14 is liquefied and expanded -> 143K

The Biggest disadvantage of the method is the use of several compressor units, which makes the system noisy and bulky. Consecutive compression cycles are replaced by a single compressor loop in the so-called *Joule Thomson –Refrigeration* (JT) method used in our home made scheme.

A semi-cryogenic system was developed with the JT-method (Fig. 19). The cooling system is based on the JT-effect can be easily explained: a highly compressed gas, upon its expansion, will cool an expansion. With the recuperative

heat exchanger warm gas (3) will pre-cooled by the cold gas (6), so that an iterative process starts. The temperature in the cold head decreases. This method has the same advantages as the vapour-compression cascade refrigeration but requires only a single compressor.

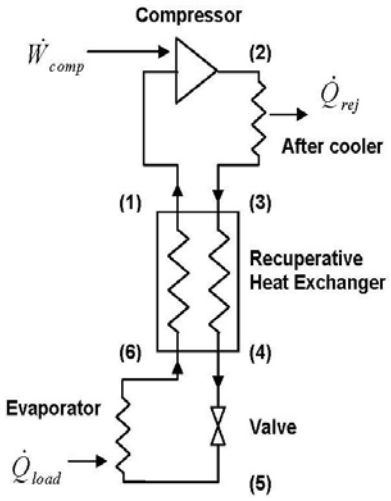

Fig. 19. The working diagram of the JT cooler that served as a blueprint for the system developed at TU WIEN for this project.

The development of the cooling unit required an extensive trial and error performance optimization by:

- Checking different gases (R404A, R23, R14, R50,R704, R740,R704)
- Different cooling powers (30W, 50W, 100W, 150W)
- Semi cryogenic-temperature stability
- Ambient temperature stability

Figure 20 shows the images of the newly developed cooling scheme.

Fig 20. 150 W 130 K JT cooler developed at TU WIEN. Insets show the photograph of the cold head that is flanged to a chamber using an ISO KF 50 flange. The inset on the right shows the design of a specially adapted crystal holder that should enable adjustable crystal clamping on four sides and minimize the exposure of the heatsink to ASE radiation.

At the time of this report, the in-house developed Joule Thomson –refrigeration unit is undergoing tests awaiting the completion of a designated miniature vacuum chamber. Figure 21 shows the cooling capacity measured at different thermal loads applied to the cold finger (Fig. 20, middle) *in air*, i.e. without vacuum thermal insulation, which proves the incredible robustness of the developed device.

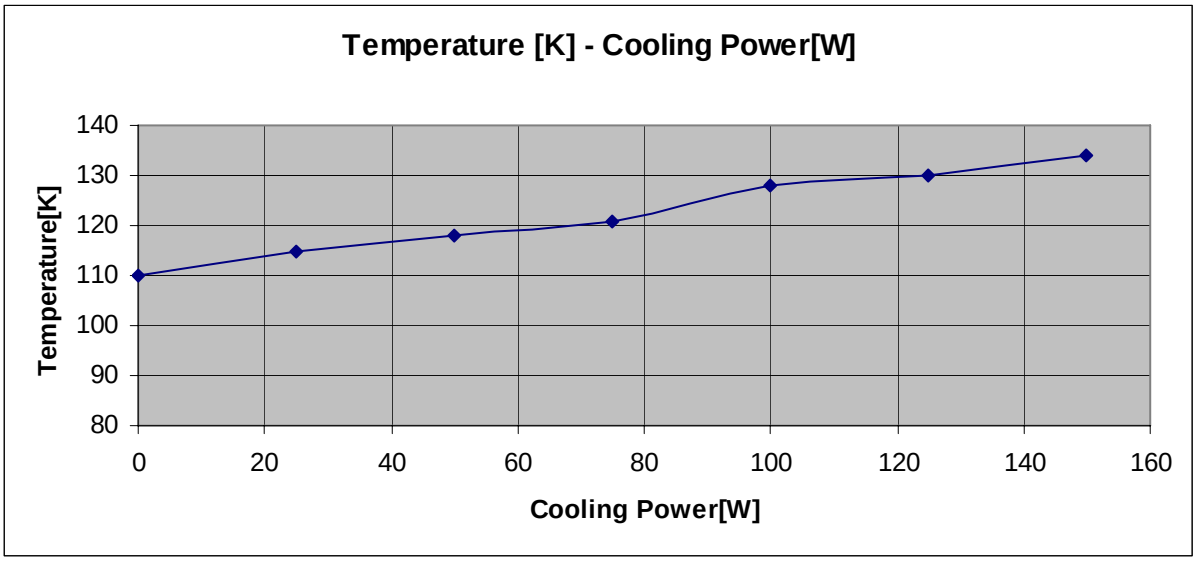

Fig 21. Measurement of the cooling power of the in-house developed JT cooler proving its suitability for Yb laser systems pumped on the order of 1 kW of optical pump power.

A semi-cryogenic system was developed with the JT-method. The cooling system is based on the JT-effect which is almost well known: Gas which is highly compressed expanded with a expansion valve cools down. With the recuperative heat exchanger warm gas (3) will pre-cooled by the cold gas (6), so that an iterative process starts. The temperature in the cold head decreases.
This method has the same advantages like the vapour-compression cascade refrigeration
with the big advantage of only one compressor.

5_ CONCLUSIONS

In this deliverable:

- we demonstrate a laser gain module designed for amplification of broadband 1030 nm pulses to a 100 mJ level and beyond. Significant technical challenges related to crystal cooling and pumping configurations have been overcome. A novel dedicated cooling system taking full advantages of the spectroscopic and mechanical properties of the laser gain crystal, Yb:CaF_2 has been designed.
- With the very encouraging results obtained during the first 12 months of the project, we are now set to complete the design of the entire 100-mJ using a cutting-edge cooling technology that can be realized in a surprisingly compact format.

6 LITERATURE, PUBLICATIONS

[Bou08] J. Boullet, Y. Zaouter, R. Desmarchelier, M. Cazaux, F. Salin, J. Saby, R. Bello-Doua and E. Cormier, "High power ytterbium-doped rod-type three-level photonic crystal fiber laser," Optics Express, 16, 17891-17902 (2008)

[Boy62] G. Boyd, R. Collins, S. Porto, A. Yariv, and W. Hargreaves, "Excitation, relaxation, and continuous maser action in the 2.613-micron transition of $CaF_2:U^{3+}$," *Phys. Rev. Lett.*, 8, 269-272, (1962).

[Cam07] P. Camy, J. L. Doualan, A. Benayad, M. v. Edlinger, V. Menard, and R. Moncorge, "Comparative spectroscopic and laser properties of Yb3+-doped CaF2, SrF2 and BaF2 single crystals," Appl. Phys. B **89,** 539–542 (2007).

[Dou07] J. L. Doualan, P. Camy, R. Moncorger, E. Daran, M. Couchaud, and B. Ferrand, "Latest developments of bulk crystals and thin films of rare-earth doped CaF2 for laser applications," Journal of Fluorine Chemistry **128,** 459–464 (2007).

[Fan90] T. Y. Fan and A. Sanchez, "Pump source requirements for end-pumped lasers", *IEEE J. Quantum Electron.*, 26, 311, (1990).

[Key64] R. J. Keyes and T. M. Quist, "Injection luminescent pumping of $CaF_2:U^{3+}$ with GaAa diode lasers," *Appl. Phys. Lett.*, 4, 59, (1964).

[Krup00] W. F. Krupke, "Ytterbium solid-state lasers: the first decade", *IEEE J. Sel. Top. Quantum Electron.*, 6, 1287, (2000).

[Luc04] A. Lucca, M. Jacquemet, F. Druon, F. Balembois, P. Georges, P. Camy, J. L. Doualan, and R. Moncorge, "High-power tunable diode-pumped Yb3+:CaF2 laser," Opt. Lett. **29,** 1879-1881 (2004).

[Pug09] A. Pugžlys, G. Andriukaitis, D. Sidorov, A. Irshad, A. Baltuška, W.J. Lai, P.B. Phua, L. Su, J. Xu, H. Li, R. Li, S. Ališauskas, A.Marcinkevičius, M.E. Fermann, L. Giniūnas, R. Danielius, "Spectroscopy and lasing of cryogenically cooled Yb, Na:CaF2", *Appl. Phys. B* 97, 339-350 (2009).

[Pug09a] A. Pugžlys, G. Andriukaitis, A. Baltuška, L. Su, J. Xu, H. Li, R. Li, W. J. Lai, P. B. Phua, A. Marcinkevičius, M. E. Fermann, L. Giniūnas, R. Danielius, S. Ališauskas, Multi-mJ, 200-fs, cw-pumped, cryogenically cooled, Yb,Na:CaF2 amplifier, Opt. Lett. **34** 2075-2077 (2009)

[Rip05] D. J. Ripin, J. R. Ochoa, R. L. Aggarwal, and T. Y. Fan, "300-W cryogenically cooled Yb:YAG laser," *IEEE journal of Quantum Electronics*, 41, 1274, (2005).

[Sie07] M. Siebold, M. Hornung, S. Bock, J. Hein, M. C. Kaluza, J.Wemans, and R. Uecker, "Broad-band regenerative laser amplification in ytterbium-doped calcium fluoride (Yb:CaF2)," Appl. Phys. B **89,** 543–547 (2007).

[Sie08] M. Siebold, M. Hornung, R. Boedefeld, S. Podleska, S. Klingebiel, C. Wandt, F. Krausz, S. Karsch, R. Uecker, A. Jochmann, J. Hein, and M. C.

Kaluza, "Terawatt diode-pumped Yb:CaF2 laser," Opt.Lett. **33,** 2770-2772 (2008).

[Sie09] M. Siebold, S. Bock, U. Schramm, B. Xu, J. L. Doualan, P. Camy, and R. Moncorgé, "Yb:CaF2—a new old laser crystal," Appl. Phys. B **97,** 327–338 (2009)

[Sor60] P. Sorokin and M. Stevenson, "Stimulated infrared emission from trivalent uranium," *Phys. Rev. Lett*, 5, 557-559, (1960).

[Su05] L. Su, J. Xu, H. Li, L. Wen, Y. Zhu, Z. Zhao, Y. Dong, G. Zhou, and J. Si, "Sites structure and spectroscopic properties of Yb-doped and Yb, Na-codoped CaF_2 laser crystals," *Chem. Phys. Lett.* 406, 254-258 (2005).

[Su05a] L. Su, J. Xun, H. Li, W. Yang, Z. Zhao, J. Si, Y. Dong, and G. Zhou, "Codoping Na^+ to modulate the spectroscopy and photoluminescence properties of Yb^{3+} in CaF_2 laser crystal," *Opt. Lett.* 30, 1003-1005, (2005).

[Web03] M. J. Weber, *Handbook of optical materials*: CRC Press LLC, (2003).